The electron affinity of the uranium atom

Sandra M. Ciborowski, [iD] Gaoxiang Liu, [iD] Moritz Blankenhorn, [iD] Rachel M. Harris, Mary A. Marshall, Zhaoguo Zhu, [iD] Kit H. Bowen, and [iD] Kirk A. Peterson

View Online   Export Citation   CrossMark

ARTICLES YOU MAY BE INTERESTED IN

The Journal of Chemical Physics

AIP Publishing
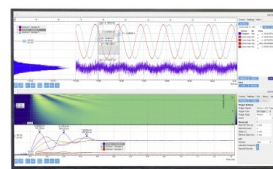
The electron affinity of the uranium atom

View Online   Export Citation   CrossMark

Sandra M. Ciborowski,[1] Gaoxiang Liu,[1] (ID) Moritz Blankenhorn,[1] (ID) Rachel M. Harris,[1] (ID) Mary A. Marshall,[1] Zhaoguo Zhu,[1] Kit H. Bowen,[1,a] (ID) and Kirk A. Peterson[2,a] (ID)

AFFILIATIONS

[1] Department of Chemistry, Johns Hopkins University, Baltimore, Maryland 21218, USA
[2] Department of Chemistry, Washington State University, Pullman, Washington 99162, USA

[a] Authors to whom correspondence should be addressed: kbowen@jhu.edu and kipeters@wsu.edu

ABSTRACT

The results of a combined experimental and computational study of the uranium atom are presented with the aim of determining its electron affinity. Experimentally, the electron affinity of uranium was measured via negative ion photoelectron spectroscopy of the uranium atomic anion, U⁻. Computationally, the electron affinities of both thorium and uranium were calculated by conducting relativistic coupled-cluster and multi-reference configuration interaction calculations. The experimentally determined value of the electron affinity of the uranium atom was determined to be 0.309 ± 0.025 eV. The computationally predicted electron affinity of uranium based on composite coupled cluster calculations and full four-component spin–orbit coupling was found to be 0.232 eV. Predominately due to a better convergence of the coupled cluster sequence for Th and Th⁻, the final calculated electron affinity of Th, 0.565 eV, was in much better agreement with the accurate experimental value of 0.608 eV. In both cases, the ground state of the anion corresponds to electron attachment to the 6d orbital.

Published under an exclusive license by AIP Publishing. https://doi.org/10.1063/5.0046315

INTRODUCTION

The actinides comprise the elements from actinium through lawrencium in the Periodic Table. In broad terms, the chemical bonding behaviors of actinium and thorium resemble those of the transition metals; the 5f valence electrons of protactinium, uranium, neptunium, and plutonium play important roles in their bonding; and among the still heavier elements, their bonding tends to mimic the lanthanide elements in terms of electron shielding and their f electron contributions.[1–13]

This work focuses on uranium and, in particular, on the electron affinity (EA) of its atom. There have been many studies of uranium, often focusing on its radioactivity, its natural decay products, the ability of certain of its isotopes to undergo nuclear fission, and their resulting fission products. Some of these aspects lead to long-term health and environmental concerns, regarding the storage and disposition of nuclear waste, which is generated by power reactors and production facilities, as well as the handling of natural uranium in mines and isotopically depleted uranium projectiles on battle-fields.[14–17] Important physical properties that have been measured include uranium's melting point, boiling point, ionization potential, and half-life, the latter being approximately the age of the Earth in the case of uranium's 238 isotope.[18–21]

Because uranium exhibits metallic bonding character under most conditions, its chemical reactions can proceed without 6d electron promotion, leading to its facile reactivity.[11] The chemistry of uranium is thus the chemistry of its oxidation products. With a ground state electron configuration of $[Xe]5f^3 6d^1 7s^2$, uranium exhibits oxidation states ranging from +3 to +6, and given the itinerant nature of uranium's 5f electrons, its chemical bonds often involve their significant contribution.[22]

Surprisingly, despite widespread interest in uranium, its electron affinity (EA) has not been measured experimentally. Computationally, however, there have been several predictions of the uranium atom's electron affinity, all of which have had to contend with strong spin–orbit and relativistic effects. These calculated electron affinities of uranium (in meV) are 175,[25] 290,[23] 300,[24] 373,[26] 531,[23] and 702,[23] with publication dates ranging from 1984 to 2009. All of these studies predict electron attachment to either the 7p or 6d orbitals of the U atom.

The work herein presents the results of a combined experimental and computational study aimed at determining the electron affinity of the uranium atom. This involved experimentally measuring the electron affinity of the uranium atom by using anion photoelectron spectroscopy and computationally predicting the EA value of uranium by conducting coupled cluster and multi-reference

configuration interaction calculations. Since an accurate experimental measurement of the electron affinity of the thorium atom has recently become available,[27] we also carried out benchmark calculations of the EA value of thorium in order to help validate our computational methods.

METHODS

Experimental

Anion photoelectron spectroscopy is conducted by crossing a beam of mass-selected negative ions with a fixed-frequency photon beam and energy analyzing the resultant photodetached electrons. The photodetachment process is governed by the energy-conserving relationship $h\nu = EBE + EKE$, where $h\nu$ is the photon energy, EBE is the electron binding (photodetachment transition) energy, and EKE is the electron kinetic energy. Our apparatus consists of a laser vaporization anion source, a time-of-flight mass spectrometer, an Nd:YAG photodetachment laser, a magnetic bottle (MB) electron energy analyzer, and a velocity-map imaging (VMI) electron energy analyzing spectrometer.[28] The magnetic bottle photoelectron spectrometer's resolution is ~35 meV at EKE = 1 eV, and the VMI spectrometer resolution is $\Delta E/E \sim 0.03$.[28] The first (1064 nm, 1.16 eV) and third (355 nm, 3.49 eV) harmonic outputs of an Nd:YAG laser were both used to photodetach electrons from mass-selected atomic uranium anions, U⁻, with the first harmonic photoelectron spectrum being energy-analyzed by the VMI spectrometer and with the third harmonic photoelectron spectrum being energy-analyzed by the MB spectrometer. The well-known atomic transitions of Cu⁻ and the molecular transitions of NO⁻ were used to calibrate the MB-measured and VMI-measured photoelectron spectra, respectively.[29,30] The atomic uranium anions were generated by a laser vaporization ion source. This device consisted of a rotating, translating depleted, i.e., pure U-238, uranium rod, which was being ablated by second harmonic (532 nm, 2.33 eV) photon pulses from an Nd:YAG laser while being bathed by synchronous high pressure pulses of high purity helium gas.

Computational

Initial studies were carried out to calculate the electron affinities of both the thorium and uranium atoms by using the full internally contracted multi-reference configuration interaction (CMRCI) level of theory[31] in order to facilitate the study of both 7p and 6d electron attachments. These calculations employed orbitals from complete active-space, self-consistent field (CASSCF) calculations using the same active-space for Th and U, i.e., the 6d, 7s, 7p, and 5f orbitals. The lower-lying orbitals were optimized but constrained to be doubly occupied. These same CAS configurations were used as the reference functions in the subsequent CMRCI calculations, where all the valence electrons were correlated (6s, 6p, 6d, 7s, 5f). The multi-reference Davidson correction was used throughout,[32] i.e., CMRCI+Q. The basis sets employed corresponded to the all-electron cc-pVXZ-DK3 sets (X = D, T, Q)[16,33] extended with an even-tempered set of diffuse functions in each angular momentum (denoted VXZ-DK+ below) in order to provide more accurate electron affinities. The third order Douglas–Kroll–Hess (DKH3) scalar relativistic Hamiltonian[34,35] was used throughout. The CASSCF

energies were extrapolated to the complete basis set (CBS) limit using[36]

$$E_n^{HF} = E_{CBS}^{HF} + A(n+1)e^{-6.57\sqrt{n}} \tag{1}$$

with VTZ-DK+ and VQZ-DK+ basis sets (n = 3, 4), and the analogous correlation energies were extrapolated to their CBS limits using[37]

$$E_n^{corr} = E_{CBS}^{corr} + \frac{B}{(n+1/2)^4}. \tag{2}$$

The results of these two extrapolations were combined to yield the total CMRCI+Q/CBS limit energies. The lowest-lying electronic terms for Th⁻ were found to be ⁴F and ⁴G°, corresponding to the electron configurations [Rn]6d³7s² and [Rn]6d²7s²7p¹, respectively. For the U⁻ atomic anion, the analogous terms were ⁶M° and ⁶M for the electron configurations [Rn]5f³6d²7s² and [Rn]5f³6d¹7s²7p¹, respectively. The neutral atom ground states correspond to ³F ([Rn]6d²7s²) and ⁵Lᵒ ([Rn]5f³6d¹7s²) for Th and U, respectively.

In the context of these multi-reference calculations, spin–orbit (SO) effects were included using the state-interacting approach at the CASSCF level of theory using the full Breit–Pauli operator.[38] The neutral atoms and anions were treated separately, and for the anion calculations, both the d- and p-attached electronic states were treated simultaneously. State-averaged orbitals were used throughout these calculations. In addition, for the Th⁻ case, the quartet G, F, D, and P states associated with the 7p¹ configuration were all included.

The Feller–Peterson–Dixon (FPD)[39–44] composite method was also used to determine the electron affinities for both the Th and U atoms. This approach has previously been successfully applied to the first few ionization potentials of lanthanide[65] and actinide[33] atoms, as well as the electron affinities of the heavy p-block elements.[66] The present calculations only focused on the lowest energy states of the negative ions, which involved electron attachment to the 6d orbitals; the numerous contributions to the electron affinities are described in detail below. The majority of these calculations were carried out at the coupled-cluster singles and doubles with perturbative triples [CCSD(T)] level of theory with the DKH3 Hamiltonian, also utilizing the diffuse-augmented VXZ-DK3+ basis sets (X = D, T, Q).[16,33] Core-valence correlation, i.e., 5s5p5d on Th and U, was also considered, and in these cases, wCVXZ-DK+ basis sets were used, i.e., cc-pwCVXZ-DK3 sets[16,33] with a series of even-tempered diffuse functions. The coupled cluster calculations employed restricted open-shell HF (ROHF) orbitals, although the spin restriction was relaxed in the CCSD(T) calculations, i.e., the R/UCCSD(T) method.[45–47] All of the CCSD(T) calculations, as well as the CMRCI calculations described above, were carried out using the MOLPRO quantum chemistry package.[48]

The final FPD electron affinities were constructed based on the following contributions to the energies:

$$E_{FPD} = E_{wCVQZ-DK+} + \Delta E_{CBS} + \Delta E_{CV} + \Delta E_{SO} + \Delta E_{Gaunt}$$
$$+ \Delta E_{Lamb} + \Delta E_T + \Delta E_Q, \tag{3}$$

where $E_{wCVQZ-DK+}$ is the total energy at the frozen-core (FC) CCSD(T)/wCVQZ-DK+ level of theory. The HF energies were then extrapolated to the CBS limit using Eq. (1) with wCVTZ-DK+ and wCVQZ-DK+ basis sets, and the analogous correlation energies were extrapolated to their CBS limits using Eq. (2). The results

of these two extrapolations were combined to yield the total FC-CCSD(T)/CBS energies, with the difference between the latter values and $E_{wCVQZ-DK+}$ yielding ΔE_{CBS}. ΔE_{CV} is the core correlation contribution, $E_{CV} - E_{valence}$, both in the same wCVXZ-DK+ basis sets ($X = T$ and Q), extrapolated to the CBS limit using Eq. (2).

Spin orbit (SO) contributions, ΔE_{SO}, were calculated using full four-component Dirac–Hartree–Fock (DHF) Kramers-restricted configuration interaction (KRCI)[49] with the Dirac–Coulomb Hamiltonian and uncontracted VTZ-DK3+ basis sets. The spin-free Hamiltonian of Dyall[50] in an analogous multireference CI (MRCI)[51] was used for comparison. The contributions from the two-electron Gaunt term, ΔE_{Gaunt}, were obtained at the four-component DHF/VTZ-DK3+ level with the Dirac–Coulomb–Gaunt Hamiltonian. The DHF calculations utilized average-of-configuration DHF orbitals involving 2–3 electrons in the 10 spinors arising from the 6d orbitals for Th/Th⁻ and 4–5 electrons in the 24 spinors arising from the 5f and 6d orbitals for U/U⁻. The KRCI/MRCI calculations for Th and Th⁻ utilized three GASs (generalized active-spaces) involving single excitations from the 6p orbital and singles and doubles from the 7s and 6d orbitals. In the cases of U and U⁻, an additional GAS was added that included singles and doubles from the 5f orbitals. A virtual orbital cutoff of 10.0 a.u. was used throughout. All SO and Gaunt calculations for Eq. (3) were carried out using the DIRAC program.[52]

ΔE_{Lamb} is a contribution for the Lamb shift or quantum electrodynamic (QED) effects. In this work, the local potential approach of Pyykkö has been used for both the vacuum polarization and self-energy contributions.[33,53] These calculations were carried out with the MOLPRO program at the FC-CCSD(T) level of theory with the wCVDZ-DK+ basis sets and DKH3 Hamiltonian.

The next two terms, ΔE_T and ΔE_Q, account for valence electron correlation effects beyond the CCSD(T) level of theory. The ΔE_T term is defined as the difference between CCSDT and CCSD(T) in the VTZ-DK3+ basis set with the DKH3 Hamiltonian.[54,55] The effect of quadruple excitations, ΔE_Q, was defined as the difference between CCSDT(Q)[56,57] and CCSDT using truncated VTZ-DK+ basis sets, where the diffuse g and h functions were not included. Calculations were also carried out on Th/Th⁻ using full iterative CCSDTQ with the smaller VDZ-DK3+ basis set, and this yielded an EA smaller by just 0.05 kcal/mol (0.002 eV) compared to CCSDT(Q) with the same basis. In the case of thorium, it was possible to also include the approximate effects of pentuple excitations, ΔE_P, as the difference between CCSDTQ(P)[58] and CCSDTQ[59,60] calculations with a truncated VDZ-DK3+ basis set (the diffuse g was deleted). The MRCC program[61] as interfaced to MOLPRO was used for all the higher-order electron correlation calculations.

RESULTS AND DISCUSSION

Experimental

The negative ions observed due to laser ablation of a depleted uranium target rod are presented in the mass spectrum shown in Fig. 1. In addition to anions of the various uranium oxides, a weak intensity of the uranium atomic anion, U⁻, was also observed.

The photoelectron spectrum of mass-selected uranium atomic anions was measured at two photon energies of an Nd:YAG laser and with two different types of electron energy analyzers: at the
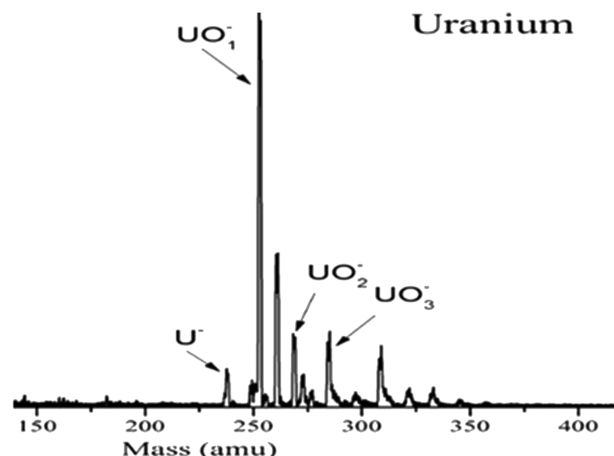

FIG. 1. Mass spectrum resulting from laser vaporization of a depleted uranium target.

third harmonic (355 nm, 3.49 eV) using our magnetic bottle (MB) spectrometer and at the first harmonic (1064 nm, 1.16 eV) using our velocity-map imaging (VMI) spectrometer. Figures 2 and 3 present these spectra, respectively. Neither of these U⁻ spectra exhibit leakage from UH⁻ photoelectron spectra nor do they exhibit transitions from potentially long-lived excited U⁻ anion states. We have separately measured the photoelectron spectrum of UH⁻ and have found that its strongest peaks are concentrated between EBE = 0.5 and 1.0 eV. That is a relatively quiet spectral region in both Figs. 2 and 3, and there is nothing above the noise level in that region, thus showing that there is no measureable leakage of UH⁻ into the photoelectron spectrum of U⁻. In addition, our computational results (see Table I) predict the lowest-lying 7p (excited) state to lie above the ground state of U⁻ by 84 meV. Based on our measured value of EA(U), this implies a photoelectron transition at EBE = 225 meV. This of course is predicated on that particular excited anion state being populated and being long-lived enough to reach a photodetachment interaction region. A second excited anion state is also expected to exist above this first one, implying a photoelectron transition at an even lower EBE. Neither putative excited state transitions
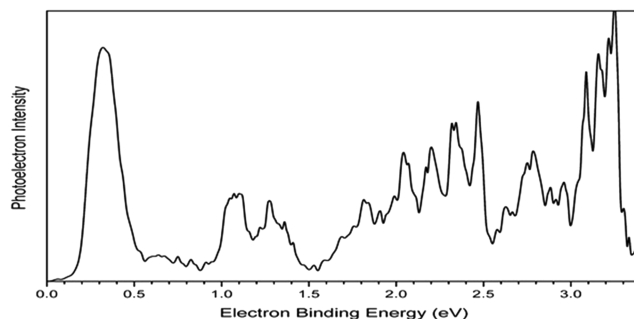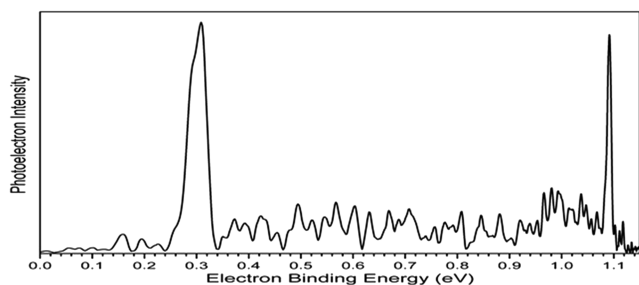

FIG. 2. Photoelectron spectrum of the uranium atomic anion (U⁻) measured with the third harmonic of an Nd:YAG laser (355 nm, 3.49 eV) and our magnetic bottle (MB) electron energy analyzer.

FIG. 3. Photoelectron spectrum of the uranium atomic anion (U⁻) measured with the first harmonic of an Nd:YAG laser (1064 nm, 1.16 eV) and our velocity-map imaging (VMI) electron energy analyzer.

are apparent in our photoelectron spectra. In Fig. 2, which exhibits lower resolution than the spectrum in Fig. 3, the spectral width of the main peak would obscure their presence if they were to be there, whereas in Fig. 3, there is nothing above the noise level in the subject spectral regions, with these observations implying that excited anion transitions do not play a significant role in those spectra. For atomic anions with no electronic hot bands, the electron binding energy (EBE) at the intensity maximum of the lowest-lying EBE peak corresponds to the electron affinity (EA) of the atom, where the EA is defined as the energy difference between the ground state of the anion and the ground state of its neutral counterpart.

The electron binding energy of the fitted intensity maximum of the lowest EBE peak in Fig. 2 is located at 0.290 eV, with this corresponding to the electron affinity of the uranium atom. Based on the instrumental resolution of our magnetic bottle analyzer at the electron kinetic energy of the lowest EBE peak and on its FWHM, we assign an error of ±0.100 eV to this measurement. Beyond the lowest EBE peak, the higher EBE peaks in this spectrum are due to photodetachment transitions from the ground state of the uranium atomic anion to the many electronic excited states of the neutral uranium atom. The previously unknown spectrum of U⁻ in Fig. 2 is what the U⁻ photoelectron spectrum looks like over the reported EBE range and at the resolution of our magnetic bottle analyzer. The transitions observed in this spectrum are also compared with the NIST atomic levels for the uranium atom in Fig. S1 of the supplementary material. While the NIST transitions are from optical spectra, our photoelectron spectrum recovers dark states as well.

The electron binding energy of the fitted intensity maximum of the lowest EBE peak in Fig. 3 is located at 0.309 eV, with this corresponding to the photodetachment transition from the ground electronic state of the uranium atomic anion to the ground electronic

state of the neutral uranium atom and thus to the electron affinity of the uranium atom. While the signal-to-noise ratio in Fig. 3 is lower than that in Fig. 2, the resolution of the VMI analyzer is significantly higher than that of the MB analyzer. Based on the instrumental resolution of our VMI electron energy analyzer and the FWHM of the lowest EBE peak, we assign an error of ±0.025 eV to this measurement. Beyond the lowest EBE peak at EBE = 0.309 eV, there is a higher EBE peak at EBE = 1.091 eV. This is the photodetachment transition from the electronic ground state of the uranium atomic anion to the first electronically excited state of the neutral uranium atom corresponding to an s electron detachment. While all atomic photodetachment transitions are inherently narrow, this peak is sharper than the origin-containing (lowest EBE) peak because the instrumental resolution is better for transitions at lower electron kinetic energies. The energy difference between this well-defined peak and the lowest EBE peak is the energy splitting between the ground state of the neutral uranium atom ($^5L_6^o$), having the configuration $5f^3(^4I^o)6d7s^2$ and the $5f^3(^4I^o)6d^2(^2F)7s$ ($^7M_6^o$) excited state of the neutral uranium atom. According to NIST, CNRS, and NBS energy level tables,[62–64] this energy separation is 6249 cm⁻¹ or 0.775 eV. In Fig. 3, this spitting, i.e., 1.091–0.309 eV, is 0.782 eV, well within the stated error bar. One of our VMI (raw) images is shown in Fig. S2 of the supplementary material.

The electron affinity of the uranium atom, EA(U), was determined to be 0.290 ± 0.100 eV using the magnetic bottle electron energy analyzer and 0.309 ± 0.025 eV using the VMI electron energy analyzer. While both of these measurements are consistent with one another, the VMI determination is easily the more accurate of the two, leading to 0.309 ± 0.025 eV as our reported value for the electron affinity of the uranium atom.

MRCI calculations of the electron affinities of Th and U

Table I shows the results of the CMRCI+Q calculations for the electron affinities of both uranium and thorium. In each case, the ground state of the anion involves electron attachment to the 6d orbital rather than the 7p orbital in agreement with most previous studies. Without the inclusion of spin–orbit effects, electron attachment to the 7p orbital is unstable in both cases. Clearly, the electron affinity of thorium is much larger than that of uranium, 13.5 kcal/mol (0.585 eV) vs 3.9 kcal/mol (0.169 eV), before SO effects are accounted for. As expected, SO has the largest effect on the electron binding to the 7p orbital, which results in the 7p-attached states being stable with respect to loss of an electron. For Th⁻, the $6d^2 7s^2 7p^1$ ($^4G_{5/2}^o$) state is still higher in energy than the ground $6d^3 7s^2$ ($^4F_{3/2}$) state by 5.8 kcal/mol (0.25 eV) at this level of

TABLE I. CMRCI+Q calculations of the electron affinities of Th and U (in kcal/mol with meV in parentheses).

Atom	Anion state	VTZ-DK+	VQZ-DK+	CBS	CBS+SO
Th	$^4F_{3/2}$ ($6d^3 7s^2$)	12.78	13.22	13.47	11.94 (518)
	$^4G_{5/2}^o$ ($6d^2 7s^2 7p^1$)	−1.23	−1.27	−1.29	6.12 (265)
U	$^6M_{13/2}^o$ ($5f^3 6d^2 7s^2$)	3.35	3.72	3.93	4.80 (208)
	$^6M_{13/2}$ ($5f^3 6d^1 7s^2 7p^1$)	−2.82	−2.90	−2.94	2.86 (124)

theory. The previous calculations of Tang et al.[27] using the multi-configurational Dirac–Hartree–Fock (MCDHF) method predicted a much smaller energy difference of just 1.1 kcal/mol (0.048 eV). In the case of U⁻, the calculations of this work predict that the $5f^3 6d^1 7s^2 7p^1$ ($^6M_{13/2}$) state lies higher than $5f^3 6d^2 7s^2$ ($^6M^o_{13/2}$) by 1.9 kcal/mol (0.082 eV). From the MCDHF calculations of O'Malley and Beck, an additional 7p state of U⁻, $^6L_{11/2}$, may lie slightly below the detachment threshold, but if their relative energy between the $^6M_{13/2}$ and $^6L_{11/2}$ states (182 meV) is applied to the results of this work, it would lie well above the threshold. At the present FC-MRCI+Q/CBS + SO level of theory, the EA values for Th and U are both smaller with respect to experiment by about 2 kcal/mol (~90 meV).

Composite coupled cluster results for the Th and U electron affinities

The individual energy contributions to the electron affinities of both thorium and uranium, within the coupled cluster FPD scheme, are presented in Table II. These calculations focus only on the ground states of the atoms, neutral and anion. Overall, the contributions not involving SO coupling are remarkably similar between the two atoms. In both cases, the FC-CCSD(T) electron affinities are well converged with respect to the basis set at the QZ level. Upon comparison to Table I, CMRCI+Q and CCSD(T) differ at their FC CBS limits by 1.1 kcal/mol (48 meV) and 1.4 kcal/mol (61 meV) for Th and U, respectively, with the CMRCI+Q values being smaller in both cases. It should be noted that the CCSD(T) calculations on U and U⁻ were very sensitive to the specific symmetry-broken electronic states chosen for the ROHF calculations. While the various coupled cluster diagnostics, e.g., the T_1 diagnostic (0.023 for U and 0.042 for U⁻), did not reflect strong multireference character, the resulting energies were very sensitive to these choices, with resulting EAs differing by many kcal/mol. In the present calculations, the states chosen and used throughout corresponded to those giving the lowest CCSD(T) total energies with the VTZ-DK+ basis set. An additional cautionary indicator in the CCSD calculations for U was the relatively large value of two doubles amplitudes, 0.127, whereas there were no doubles amplitudes above 0.056 for any of the other atoms. Correlation of the 5s, 5p, and 5d electrons with CCSD(T) reduces the electron affinities of both Th and U by just over 1 kcal/mol (43 meV). Curiously, in the recent MCDHF calculations of Tang et al.[27] for the EA of thorium, where agreement with experiment to within 0.2 kcal/mol (8 meV) was presented, correlation of these electrons was not included. Hence, this excellent agreement may have been somewhat fortuitous. In this work, the inclusion of spin–orbit

coupling, including small effects due to the Gaunt interaction, decreases the electron affinity of thorium by about 1 kcal/mol (43 meV), while in the case of uranium, the inclusion of spin–orbit coupling increases the EA by a little more than 1 kcal/mol. (43 meV). The effect of the Lamb shift is identical in both cases and raises their electron affinities by just 0.3 kcal/mol (13 meV). Valence correlation effects beyond CCSD(T) are calculated to be very modest with a well-behaved convergence for the EA of Th; the values of ΔE_T, ΔE_Q, and ΔE_P for its EA were calculated to be just −0.4, +0.7, and +0.1 kcal/mol (−17, +30, and +4 meV), respectively. In the case of uranium, the values of ΔE_T and ΔE_Q were also calculated to be small, −0.4 and 0.0 kcal/mol, (−17 meV and 0 meV) respectively, but the CCSDT calculations suffered from very poor convergence, particularly for the anion calculations. Convergence could not be achieved for CCSDTQ, which prevented the use of CCSDTQ(P) for this atom. In addition, while the incremental correlation energy recovery was smoothly converging in Th and Th⁻ as the coupled cluster sequence increased in order, e.g., in Th⁻, the values of ΔE_T, ΔE_Q, and ΔE_P were −0.79, +0.50, and −0.19 mE$_h$, respectively, the values of ΔE_T and ΔE_Q for U⁻ were much larger at −6.05 and −7.03 mE$_h$, respectively, where the symbol mE$_h$ refers to milli-Hartees. This suggests that the coupled cluster sequence for the U EA is clearly not converged.

The final FPD electron affinity value for thorium, 13.04 kcal/mol (565 meV), is smaller than the accurate experimental value by just under 1 kcal/mol (43 meV). Note that if the CV contribution is omitted, nearly perfect agreement with experiment is achieved (616 vs 608 meV), which is consistent with the previous work of Tang et al.[27] Given the extensive correlation treatment and reliability of coupled cluster for Th/Th⁻, the likely largest source of error is the treatment of SO coupling, which was carried out at the KRCI level of theory. It should be noted that correlation effects on the SO contribution raised the electron affinity of both thorium and uranium. The final electron affinity of uranium, 5.34 kcal/mol (232 meV), is presumably also under-estimated due to a similar treatment of SO but is also expected to suffer larger errors due to a less accurate treatment of electron correlation effects. In fact, the EA$_{FPD}$ value of 5.34 kcal/mol (232 meV) is indeed lower than the electron affinity value that was determined experimentally in this work (7.13 kcal/mol or 309 meV) by 1.8 kcal/mol (77 meV), and this is nearly twice as large as the analogous difference for the Th EA. Similar to the Th⁻ case, if the CV contribution is omitted, the resulting EA (281 meV) is in much better agreement with experiment. The most accurate previous calculation of the EA of U, the relativistic MRCI calculations of O'Malley and Beck,[26] yielded a 6d attachment EA of 260 meV (6.00

TABLE II. Calculated contributions to the electron affinities (in kcal/mol) within the coupled cluster FPD scheme. See Eq. (3) for details. Values in meV are given in parentheses.

Atom	$E_{wCVQZ-DK+}$	ΔE_{CBS}	ΔE_{CV}	ΔE_{SO}[a]	ΔE_{Gaunt}	ΔE_{Lamb}	ΔE_T	ΔE_Q	ΔE_P	E_{FPD}	Expt.
Th	14.26	+0.29	−1.17	−1.30	+0.28	+0.28	−0.37	+0.69	+0.08	13.04	14.01[b]
	(618)	(+13)	(-51)	(-56)	(+12)	(+12)	(-16)	(+30)	(+3)	(565)	(608)[b]
U	5.06	+0.25	−1.13	+1.14	+0.14	+0.28	−0.42	+0.01	. . .	5.34	7.13[c]
	(219)	(+11)	(-49)	(+49)	(+6)	(+12)	(-18)	(+0.4)	. . .	(232)	(309)[c]

[a]The corresponding average-of-configuration DHF values were −1.66 and +0.06 kcal/mol (−71 and +3 meV) for Th and U, respectively.
[b]Photoelectron imaging value of Ref. 27, 14.0137 ± 0.0014 kcal/mol (607.692 ± 0.061 meV).
[c]This work, 7.13 ± 0.58 kcal/mol (309 ± 25 meV).

kcal/mol), which is in better agreement with the present experimental value, but as with the Th EA calculations of Tang *et al.*,[27] the work of O'Malley and Beck did not correlate the 5d electrons; in addition, they also neglected correlation of the 6p electrons. This could be why the latter work also incorrectly (according to this work) predicted the ground state of U$^-$ to correspond to a 7p attachment with an EA of 373 meV (8.60 kcal/mol). Their calculations had similar problems with the EA of the Th atom, predicting a 7p attachment EA of 368 meV and a 6d attachment EA of 304 meV. The latter is in error relative to the accurate experiment of Tang *et al.*[27] by a factor of 2.

CONCLUSIONS

The electron affinity of the uranium atom has been determined as 0.309 eV ± 0.025 eV using anion photoelectron spectroscopy. Extensive MRCI calculations predict that the electron affinity corresponds to the electron attachment to the 6d orbital rather than to the 7p orbital, which is similar to the Th atom case. Even though the composite coupled cluster method used in this work was not deemed as accurate for the EA of U as for Th, the final calculated value of 232 meV was still in better agreement with the new experimental value compared to calculations based on MRCI. The EA of U represents a significant challenge for relativistic correlation methods. The analogous coupled-cluster-based result for the EA of Th in this work, 565 meV, differed from experiment by just 43 meV, where most of the residual error is proposed to arise from incomplete recovery of SO effects.

SUPPLEMENTARY MATERIAL

See the supplementary material for Figs. S1 and S2.

AUTHORS' CONTRIBUTIONS

S.M.C., G.L., M.B., R.M.H., M.A.M., and Z.Z. participated in the anion photoelectron spectroscopic measurements. K.A.P. performed the theoretical calculations. K.H.B. supervised the experimental work. S.M.C., K.A.P., and K.H.B. drafted the manuscript.

Note added in proof. During the proof stage it was brought to the authors' attention that the U atom EA had recently been reported by Tang *et al.*, Phys. Rev. A **103**, L050801 (2021).

DATA AVAILABILITY

The data that support the findings of this study are available from the corresponding authors upon reasonable request.

REFERENCES

[1] J. K. Gibson, Int. J. Mass Spectrom. **214**, 1 (2002).
[2] B. Johansson, Phys. Rev. B **11**, 2740 (1975).
[3] M. O. Krause, R. G. Haire, O. Keski-Rahkonen, and J. R. Peterson, J. Electron Spectrosc. **47**, 215 (1988).
[4] F. David, K. Samhoun, R. Guillaumont, and N. Edelstein, J. Inorg. Nucl. Chem. **40**, 69 (1978).
[5] R. G. Haire, J. Alloys Compd. **223**, 185 (1995).
[6] L. Petit, A. Svane, W. M. Temmerman, and Z. Szotek, Solid State Commun. **116**, 379 (2000).
[7] B. Johansson and H. L. Skriver, J. Magn. Magn. Mater. **29**, 217 (1982).
[8] P. G. Huray, S. E. Nave, and R. G. Haire, J. Less-Common Met. **93**, 293 (1983).
[9] K. Wendt, T. Gottwald, C. Mattolat, and S. Raeder, Hyperfine Interact. **227**, 55 (2014).
[10] T. Moeller, J. Chem. Educ. **47**, 417 (1970).
[11] N. M. Edelstein and L. R. Morss, *Radiochemistry and Nuclear Chemistry* (Eolss Publishers, Oxford, UK, 2009), Vol. II, p. 118.
[12] L. R. Morss, N. M. Edelstein, and J. Fuger, *The Chemistry of the Actinide and Transactinide Elements* (Springer, Dordrecht, 2010).
[13] J. J. Katz and E. Rabinowitch, *The Chemistry of Uranium* (McGraw-Hill, New York, 1951).
[14] B. Villemant, *Elements: Actinide Series in Geochemistry. Encyclopedia of Earth Science* (Springer, Dordrecht, 1998).
[15] P. C. Burns and R. Finch, *Uranium: Mineralogy, Geochemistry and the Environment* (Mineralogical Society of America, Washington, DC, 1999).
[16] J. G. Hamilton, Rev. Mod. Phys. **20**, 718 (1948).
[17] E. S. Craft, A. W. Abu-Qare, M. M. Flaherty, M. C. Garofolo, H. L. Rincavage, and M. B. Abou-Donia, J. Toxicol. Environ. Health, Part B **7**, 297 (2010).
[18] J. Marcalo and J. K. Gibson, *Handbook on the Physics and Chemistry of Rare Earths* (Elsevier, Amsterdam, 2014).
[19] H. L. Skriver, O. K. Andersen, and B. Johansson, Phys. Rev. Lett. **41**, 42 (1978).
[20] G. R. Hertel, J. Chem. Phys. **47**, 335 (1967).
[21] W. Potzel, J. Moser, L. Asch, and G. M. Kalvius, Hyperfine Interact. **13**, 175 (1983).
[22] S. Cotton, *Lanthanide and Actinide Chemistry* (John Wiley & Sons, West Sussex, 2006).
[23] Y. Guo and M. A. Whitehead, Phys. Rev. A **40**, 28 (1989).
[24] S. G. Bratsch and J. J. Lagowski, Chem. Phys. Lett. **107**, 136 (1984).
[25] K. Dinov and D. Beck, Phys. Rev. A **52**, 2632 (1995).
[26] S. M. O'Malley and D. R. Beck, Phys. Rev. A **80**, 032514 (2009).
[27] R. Tang, R. Si, Z. Fei, X. Fu, Y. Lu, T. Brage, H. Liu, C. Chen, and C. Ning, Phys. Rev. Lett. **123**, 203002 (2019).
[28] G. Liu, S. M. Ciborowski, and K. H. Bowen, J. Phys. Chem. A **121**, 5817 (2017).
[29] J. Ho, K. M. Ervin, and W. C. Lineberger, J. Chem. Phys. **93**, 6987 (1990).
[30] M. J. Travers, D. C. Cowles, and G. B. Ellison, Chem. Phys. Lett. **164**, 449 (1989).
[31] K. R. Shamasundar, G. Knizia, and H.-J. Werner, J. Chem. Phys. **135**, 054101 (2011).
[32] S. R. Langhoff and E. R. Davidson, Int. J. Quantum Chem. **8**, 61 (1974).
[33] K. A. Peterson, J. Chem. Phys. **142**, 074105 (2015); R. Feng and K. A. Peterson, *ibid.* **147**, 084108 (2017).
[34] M. Douglas and N. M. Kroll, Ann. Phys. **82**, 89 (1974).
[35] M. Reiher and A. Wolf, J. Chem. Phys. **121**, 10945 (2004).
[36] A. Karton and J. M. L. Martin, Theor. Chem. Acc. **115**, 330 (2006).
[37] J. M. L. Martin, Chem. Phys. Lett. **259**, 669 (1996).
[38] A. Berning, M. Schweizer, H.-J. Werner, P. J. Knowles, and P. Palmieri, Mol. Phys. **98**, 1823 (2000).
[39] D. Feller, K. A. Peterson, and D. A. Dixon, J. Chem. Phys. **129**, 204105 (2008).
[40] K. A. Peterson, D. Feller, and D. A. Dixon, Theor. Chem. Acc. **131**, 1079 (2012).
[41] D. A. Dixon, D. Feller, and K. A. Peterson, *Annual Reports in Computational Chemistry* (Elsevier, Amsterdam, 2012), Vol. 8, p. 1.
[42] D. Feller, K. A. Peterson, and D. A. Dixon, Mol. Phys. **110**, 2381 (2012).
[43] M. Vasiliu, K. A. Peterson, J. K. Gibson, and D. A. Dixon, J. Phys. Chem. A **119**, 11422 (2015).
[44] D. Feller, K. A. Peterson, and D. A. Dixon, *Annual Reports in Computational Chemistry* (Elsevier, Amsterdam, 2016), Vol. 12, p. 47.
[45] G. E. Scuseria, Chem. Phys. Lett. **176**, 27 (1991).
[46] J. D. Watts, J. Gauss, and R. J. Bartlett, J. Chem. Phys. **98**, 8718 (1993).
[47] P. J. Knowles, C. Hampel, and H. J. Werner, J. Chem. Phys. **99**, 5219 (1993).

[48]H.-J. Werner, P. J. Knowles, G. Knizia, F. R. Manby, and M. Schütz, Wiley Interdiscip. Rev.: Comput. Mol. Sci. **2**, 242–253 (2012); H.-J. Werner, P. J. Knowles, G. Knizia, F. R. Manby, M. Schütz, P. Celani, W. Györffy, D. Kats, T. Korona, R. Lindh, A. Mitrushenkov, G. Rauhut, K. R. Shamasundar, T. B. Adler, R. D. Amos, S. J. Bennie, A. Bernhardsson, A. Berning, D. L. Cooper, M. J. O. Deegan, A. J. Dobbyn, F. Eckert, E. Goll, C. Hampel, A. Hesselmann, G. Hetzer, T. Hrenar, G. Jansen, C. Köppl, S. J. R. Lee, Y. Liu, A. W. Lloyd, Q. Ma, R. A. Mata, A. J. May, S. J. McNicholas, W. Meyer, T. F. Miller III, M. E. Mura, A. Nicklass, D. P. O'Neill, P. Palmieri, D. Peng, K. Pflüger, R. Pitzer, M. Reiher, T. Shiozaki, H. Stoll, A. J. Stone, R. Tarroni, T. Thorsteinsson, M. Wang, and M. Welborn, MOLPRO, version 2019.2, a package of *ab initio* programs, see https://www.molpro.net.

[49]T. Fleig, J. Olsen, and L. Visscher, J. Chem. Phys. **119**, 2963 (2003).

[50]K. G. Dyall, J. Chem. Phys. **100**, 2118 (1994).

[51]J. Olsen, P. Jørgensen, and J. Simons, Chem. Phys. Lett. **169**, 463 (1990).

[52]DIRAC, a relativistic *ab initio* electronic structure program, Release DIRAC19, 2019, written by A. S. P. Gomes, T. Saue, L. Visscher, H. J. Aa. Jensen, and R. Bast, with contributions from I. A. Aucar, V. Bakken, K. G. Dyall, S. Dubillard, U. Ekström, E. Eliav, T. Enevoldsen, E. Faßhauer, T. Fleig, O. Fossgaard, L. Halbert, E. D. Hedegård, T. Helgaker, B. Helmich-Paris, J. Henriksson, M. Iliaš, Ch. R. Jacob, S. Knecht, S. Komorovský, O. Kullie, J. K. Lærdahl, C. V. Larsen, Y. S. Lee, H. S. Nataraj, M. K. Nayak, P. Norman, G. Olejniczak, J. Olsen, J. M. H. Olsen, Y. C. Park, J. K. Pedersen, M. Pernpointner, R. Di Remigio, K. Ruud, P. Sałek, B. Schimmelpfennig, B. Senjean, A. Shee, J. Sikkema, A. J. Thorvaldsen, J. Thyssen, J. van Stralen, M. L. Vidal, S. Villaume, O. Visser, T. Winther, and S. Yamamoto, see http://www.diracprogram.org.

[53]P. Pyykkö and L.-B. Zhao, J. Phys. B: At., Mol. Opt. Phys. **36**, 1469 (2003).

[54]J. Noga and R. J. Bartlett, J. Chem. Phys. **86**, 7041 (1987).

[55]J. D. Watts and R. J. Bartlett, J. Chem. Phys. **93**, 6104 (1990).

[56]T. D. Crawford and J. F. Stanton, Int. J. Quantum Chem. **70**, 601 (1998).

[57]S. A. Kucharski and R. J. Bartlett, J. Chem. Phys. **108**, 5243 (1998).

[58]M. Kállay and J. Gauss, J. Chem. Phys. **123**, 214105 (2005).

[59]S. A. Kucharski and R. J. Bartlett, Theor. Chim. Acta **80**, 387 (1991).

[60]N. Oliphant and L. Adamowicz, J. Chem. Phys. **94**, 1229 (1991).

[61]MRCC, a quantum chemical program suite (see also Z. Rolik, L. Szegedy, I. Ladjánszki, B. Ladóczki, and M. Kállay, "An efficient linear-scaling CCSD(T) method based on local natural orbitals," J. Chem. Phys. **139**, 094105 (2013), as well as: www.mrcc.hu).

[62]National Institute of Standards and Technology, *Handbook of Basic Atomic Spectroscopic Data, NIST Standard Reference Database 108* (NIST, Gaithersburg, MD, 2013), https://www.nist.gov/pml/handbook-basic-atomic-spectroscopic-data; accessed 11 January 2021.

[63]J. Blaise and J. F. Wyart, *Selected Constants Energy Levels and Atomic Spectra of Actinides* (Centre National de la Recherche Scientifique, 1992), http://www.lac.u-psud.fr/old-lac/lac/Database/Contents.html; accessed 11 January 2021.

[64]C. C. Kiess, C. J. Humphreys, and D. D. Laun, J. Res. Nat. Bur. Stand. **37**, 57 (1946).

[65]Q. Lu and K. A. Peterson, J. Chem. Phys. **145**, 054111 (2016).

[66]B. A. Finney and K. A. Peterson, J. Chem. Phys. **151**, 024303 (2019); **151**, 159901 (2019).